PCCP

ROYAL SOCIETY OF CHEMISTRY

COMMUNICATION

View Article Online
View Journal | View Issue

Cite this: *Phys. Chem. Chem. Phys.*, 2021, **23**, 19146

Received 1st July 2021,
Accepted 18th August 2021

DOI: 10.1039/d1cp02980k

rsc.li/pccp

The unified quantum mechanical structure of tubular molecular rotors with multiple equivalent global minimum structures: the 18*C_{2h} → D_{9d} case of La-[B_2@B_{18}]-La†

Xiao-Qin Lu,[ab] Yuan Man,[ac] Vincent Ruß,[d] Yonghong Xu,[a] Yonggang Yang *[ac] and Si-Dian Li *[b]

La-[B_2@B_{18}]-La demonstrates decisive changes of the properties of molecular rotors, from multiple (here 18) equivalent individual global minimum structures to a quantum mechanical unified structure. This affects their geometries, their symmetries (18*C_{2h} → D_{9d}), the generation of energy bands, and high-resolution spectroscopy.

Recently, tubular molecular rotors have been discovered as a new class of molecular rotors[1–3] in addition to fluxional planar boron rotors.[4–13] A prominent example is the bi-decker tubular inverse sandwich complex La-[B_2@B_{18}]-La.[1] This rotor possesses a La-B_2-La rhombus with B–B and La–La as the short and long axes, respectively. The B_2-bar serves as the molecular "wheel" that rotates almost freely about the La–La-"axis" in its tubular B_{18}-"bearing". The formation energy of the tubular rotor La-[B_2@B_{18}]-La from its fragments La_2B_2 and B_{18} is 1270.64 kJ mol^{-1}, *i.e.*, it is stable, in spite of its fluxionality. The motif of the molecular "wheel rotating in its bearing" is somewhat analogous to planar boron rotors.[14–17] The general interest in molecular rotors is motivated by applications in molecular devices such as molecular motors.[18–21] In the realm of boron chemistry,[22,23] this Communication exemplifies the unified quantum mechanical consequences of equal probabilities and interactions of multiple equivalent global minimum structures (GMs) of metal-boron nanoclusters in the electronic ground state, in particular, for their symmetries, the vibrational energy levels, and the shaping of molecular tops. The properties of the reference GMs and the transition states (TSs) are adapted from the results of ref. 1 calculated at the PBE0 level of quantum chemistry; the quantum mechanical methods for the present extension are adapted from ref. 14; for details, see the (ESI†).

The GMs of tubular molecular rotors are characterized by optimal orientations of the wheel with respect to the tubular bearing, allowing relaxation to the structure with a minimum potential energy of $V_{GM} \equiv 0$. The bearing may offer several equivalent sites (total number = N) for optimal orientations and relaxations. As a consequence, the tubular molecular rotors have N equivalent GMs. They are characterized by specific rotation angles φ of the molecular wheel with respect to the bearing, with a cyclic order, $0^\circ < \varphi_1 < \varphi_2 < \varphi_3 < \cdots < \varphi_N < 360^\circ$ for the corresponding GM_1, GM_2, GM_3, $\cdots$, GM_N. All GMs have the same properties, except for different orientations. Two neighbouring GMs, for example GM_k and GM_{k+1}, are separated by the transition state $TS_{k,k+1}$ with a rotation angle $\varphi_{k,k+1}$ between φ_k and φ_{k+1}. Accordingly, the angular domain of GM_k is confined by its neighbouring TSs. For the N GMs, there are N TSs in the cyclic order, and all of them have the same properties, except for different orientations.

In the case of the tubular molecular rotor La-[B_2@B_{18}]-La, the tubular B_{18}-"bearing" with two staggered B_9-rings offers N = 18 equivalent sites for the optimal orientations of the B_2-"wheel". The corresponding GM_1, GM_2, GM_3, $\cdots$, GM_{18} are at $\varphi_1 = 10^\circ$, $\varphi_2 = 30^\circ$, $\varphi_3 = 50^\circ$, $\cdots$, $\varphi_{18} = 350^\circ$, separated by $TS_{1,2}$, $TS_{2,3}$, $TS_{3,4}$, $\cdots$, $TS_{18,1}$ at $\varphi_{1,2} = 20^\circ$, $\varphi_{2,3} = 40^\circ$, $\varphi_{3,4} = 60^\circ$, $\cdots$, $\varphi_{18,1} = 360^\circ \equiv 0^\circ$. Accordingly, GM_1, GM_2, GM_3, $\cdots$, GM_{18} have angular domains of (0°,20°), (20°,40°), (40°,60°), $\cdots$, (340°,360°), respectively. Three representative GMs and TSs are illustrated in Fig. 1. All GMs have the same global minimum value of a potential energy of V_{GM} = 0, the same geometry, the same C_{2h} symmetry, the same frequencies and irreducible representations (IRREPs) of the vibrational normal modes (*cf.* Fig. S3, ESI†), *etc.* As a consequence, the vibrational energy levels of GM_1, $\cdots$, GM_{18} are 18-fold degenerate. Likewise, all TSs have the same properties, *e.g.*, the same value of a potential barrier

[a] *State Key Laboratory of Quantum Optics and Quantum Optics Devices, Institute of Laser Spectroscopy, Shanxi University, Taiyuan 0300006, China. E-mail: ygyang@sxu.edu.cn*
[b] *Nanocluster Laboratory, Institute of Molecular Science, Shanxi University, Taiyuan 030006, China. E-mail: lisidian@sxu.edu.cn*
[c] *Collaborative Innovation Center of Extreme Optics, Shanxi University, Taiyuan 030006, China*
[d] *Institut für Chemie und Biochemie, Freie Universiät Berlin, 14195 Berlin, Germany*

† Electronic supplementary information (ESI) available: Details of the molecular symmetry group, the 18 equivalent GMs and TSs, and the quantum mechanical rotational/pseudo-rotational states. See DOI: 10.1039/d1cp02980k

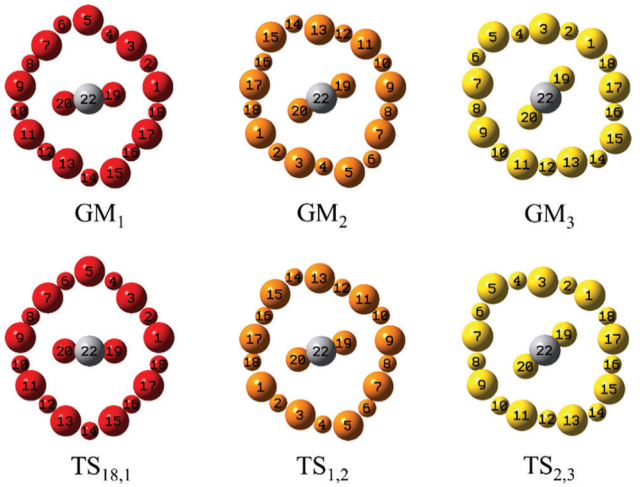

Fig. 1 Perspective views of three equivalent global minimum structures (GMs) and transition states (TSs) of the model tubular molecular rotor La-[B_2@B_{18}]-La. Nuclei in the front and in the back are illustrated by large and small balls, respectively. The z-axis with two La nuclei (grey balls, the one in the front hides the one in the back) points to the viewer. The full set of all 18 rainbow colour-coded GMs and TSs is shown in Fig. S1 and S2 (ESI†).

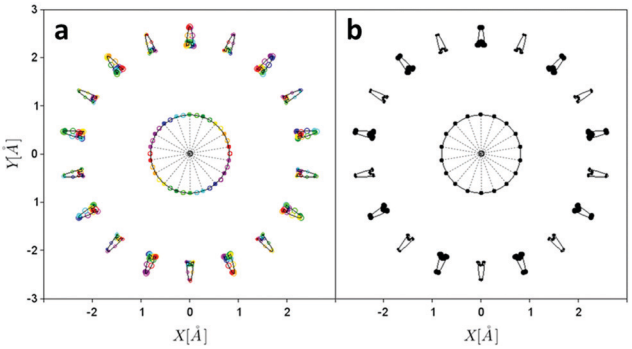

Fig. 2 (a) Perspective view of the superposition of the 18 equivalent rainbow colour-coded global minimum structures (GMs, full balls, with dashed lines for 18 central La-B_2-La rhombi) and 18 transition states (TSs, open balls) of the oriented model tubular molecular rotor La-[B_2@B_{18}]-La, *cf.* Fig. 1 and Fig. S1, S2, S4a (ESI†). (b) The quantum mechanical unified geometry of the interacting GMs, with the central double cone, *cf.* Fig. S4b (ESI†). Continuous lines guide the eyes along the nearly circular paths of the two boron nuclei of the molecular wheel and along the pseudo-rotational paths of the eighteen boron nuclei of the tubular bearing.

of $V = V_b$ = 599.27 h c cm^{-1}, the same geometry, the same C_{2h} symmetry, the same frequencies and IRREPs of the normal vibrational normal modes (*cf.* Fig. S3, ESI†), *etc.*

The purpose of this Communication was to discover the quantum mechanical consequences of equal probabilities and interactions of the equivalent GMs of tubular molecular rotors using ^{139}La-[$^{11}B_2$@$^{11}B_{18}$]-^{139}La as the example. The equivalence of the GMs is in turn the consequence of the indistinguishability of the boron nuclei; they are all fermions with a nuclear spin of 3/2$\hbar$ and a mass of 11.009u. The corresponding cyclic molecular symmetry group of all GMs is C_{18}(M), with 18 IRREPs Γ_l, $l = 0,\cdots,17$ and the cyclic graph;[24] the nuclear permutations P_1, $P_2,\cdots,P_{17}$, P_{18}(=E; $P_k = P_1^k$) for proceeding from GM$_1$ to GM$_2$, GM$_3$, …,GM$_{18}$ and finally back to GM$_1$ are listed in Table S1 (ESI†); for details, see ESI† III; see also Fig. 1 and Fig. S1 (ESI†).

To reach our goal, we employ a simple model. Specifically, we assume that the nuclear centre of mass of the oriented ^{139}La-[$^{11}B_2$@$^{11}B_{18}$]-^{139}La is at the origin of laboratory-fixed Cartesian coordinates x, y, and z, with the two metal nuclei on the z-axis ($Z_{La1} = -Z_{La2}$ = 2.398 Å). The B_2-wheel rotates about the z-axis with a radius of $R_{19} = R_{20}$ = 0.818 Å, almost perfectly in the x–y plane (alternating deviation, $\Delta Z_{19} = -\Delta Z_{20} = \pm$0.0117 Å). The two staggered B_9-rings of the tubular B_{18}-bearing, with a mean distance of 2.357 Å from the z-axis, are on opposite sides, nearly parallel to the x–y plane. The coordinates of all 2 + 18 boron nuclei of the wheel and the tubular bearing are listed in Table S2 (ESI†), for all 18 GMs and all 18 TSs.

Fig. 2a and Fig. S4a (ESI†) show the superposition of all rainbow color-coded GMs and TSs. To guide the eye, these figures include cyclic paths of all nuclei on their way from GM$_1$ *via* TS$_{1,2}$, GM$_2$, TS$_{2,3}$, GM$_3$, … to GM$_{18}$ and finally *via* TS$_{18,1}$ back to GM$_1$; see the ESI† for the mathematical construction of these paths. Apparently, the two boron nuclei of the molecular wheel rotate along φ (that means counter clockwise) in almost perfect circles, whereas the nuclei of the bearing move along the so-called cyclic pseudo-rotational paths, also counter clockwise, but phase shifted.

For simplicity, we neglect couplings between the coherent nuclear rotations/pseudo-rotations along φ and other nuclear motions. The corresponding potential energy along φ is modelled as $V(\varphi) = 0.5\ V_b\ [1 + \cos(18\varphi)]$, with the alternating potential minima ($V = 0$) and barriers ($V = V_b$) for the GMs and TSs at $\varphi_1 = 10^\circ$, $\varphi_{1,2} = 20^\circ$, $\varphi_2 = 30^\circ$, *etc.* The potential $V(\varphi)$ is illustrated in Fig. 3a, with rainbow colours corresponding to the angular domains of the GMs.

Fig. 3a also shows the $N = 18$ equivalent colour-coded localized bell-shaped wave functions $\Psi_{k0}(\varphi)$, representing the quantum mechanical rotational/pseudo-rotational ground states of GM$_k$, with energy levels E_{k0} as the base lines. Each $\Psi_{k0}(\varphi)$ is confined to the angular domain of its GM$_k$. The characteristic orientation angle φ_k of GM$_k$ is at the maximum of the density $\rho_{k0}(\varphi) = |\Psi_{k0}(\varphi)|^2$. The energy levels of E_{k0} = 103.720 h c cm^{-1} are 18-fold degenerate.

Now let us proceed from the traditional scenario of 18 equivalent individual GMs to the unified quantum mechanical image of 18 interacting GMs. In the frame of our model, the interactions of the GM$_k$ with their neighbours GM$_{k-1}$ and GM$_{k+1}$ are enabled by opening the borders between their local angular domains. As a consequence, the 18 localized $\Psi_{k0}(\varphi)$ are replaced by 18 delocalized $\Psi_{0l}(\varphi)$ which spread over the entire domain, from $\varphi = 0^\circ$ to 360°, under cyclic boundary conditions. Their energies E_{0l} are listed in Table S3 (ESI†). They form a narrow energy band, *i.e.*, they are close to each other, but no longer 18-fold degenerate. The quantum numbers 0l refer to the lowest energy band ($n = 0$) and to the IRREPs Γ_l of C_{18}(M).[15,16]

For example, Fig. 3b shows the ground state wave function $\Psi_{00}(\varphi)$ with an identity representation Γ_0, now in unicolour

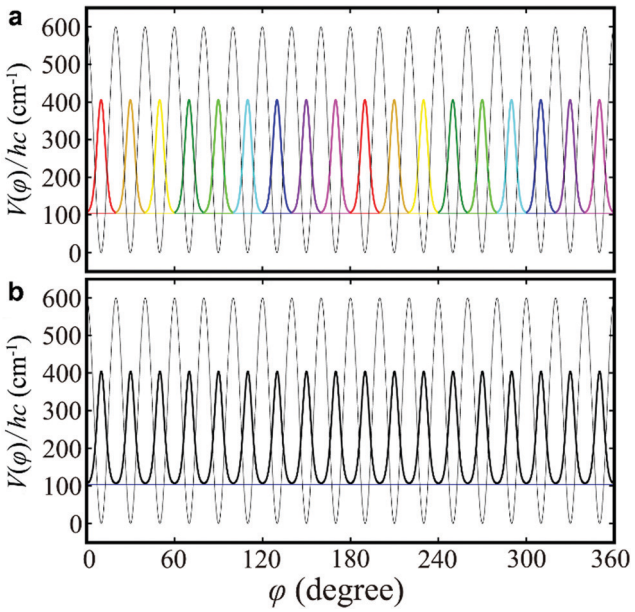

Fig. 3 (a) Rainbow colour-coded rotational/pseudo-rotational wave functions localized in the angular domains of the potential energy curve (thin grey) for the 18 global minimum structures (GMs) of the oriented model tubular molecular rotor La-[B_2@B_{18}]-La in the ground state. (b) Delocalized wave function of the rotor in the ground state (thick black), with 18 maxima indicating the equal quantum mechanical probabilities of the 18 interacting GMs. The horizontal base lines of the wave functions are at their energy levels.

(black) since it can no longer be assigned to any of the previously rainbow-coloured individual GM_k. Instead, its density $\rho_{00}(\varphi) = |\Psi_{00}(\varphi)|^2$ has 18 equivalent bell-shaped maxima which are centred at the preferential orientation angles φ_k of the equivalent GM_k. Integration of this density into the angular domains of the GM_k yields the same quantum mechanical probability (=1/18) of occupying the GM_k. Accordingly, the unified preferential quantum mechanical structure of the oriented ^{139}La-[$^{11}B_2$@$^{11}B_{18}$]-^{139}La is as shown in Fig. 2b and Fig. S4b (ESI†); it is simply the unicoloured version of GM_k as shown in Fig. 2a and Fig. S4a (ESI†), with equal quantum mechanical probabilities.

The current mechanism has fundamental consequences. (i) Structural changes: the rhombi La-B_2-La of the 18 individual GM_k (see Fig. 1, 2a and Fig. S1, S4a, ESI†) are replaced by the eighteen-cornered double cone for the 18 equally probable rotational angles of the wheel in the tubular bearing (see Fig. 2b and Fig. S4b, ESI†). (ii) Shaping of molecular tops: the principal moments of inertia I_A, I_B, and I_C (in units of uÅ^2) are changed from 2315.62, 2342.51, and 1116.02 for individual GM_k to 2279.06, 2279.06, and 1116.02, *i.e.*, the unified structure of ^{139}La-[$^{11}B_2$@$^{11}B_{18}$]-^{139}La is the prolate symmetric molecular top, whereas the individual GM_k are asymmetric tops. (iii) Elevation of symmetry: here, from C_{2h} for the 18 individual GM_k to D_{9d} ($18^*C_{2h} \rightarrow D_{9d}$). (iv) The formation of energy bands (Table S3, ESI†) by lifting the degeneracies of the levels of the individual GM_k as discussed above. A feasible way to confirm our theoretical prediction starts from the synthesis of the tubular rotor by the methods that have been developed for the production of selective La_nB_m compounds.[25–29] Then, high-resolution rotational spectroscopy[30,31] should be used to determine the three principal moments of inertia to confirm that La-[B_2@B_{18}]-La is the prolate symmetric molecular top. An alternative way might be NMR spectroscopy, which is analogous to quantum tunnelling aspects of the methyl group rotation studied by NMR.[32] More challenging experiments would be high-resolution vibrational spectroscopy to unravel the formation of energy bands.[11]

In conclusion, the quantum mechanical unification of the equivalent interacting GMs yields the unified properties of the oriented tubular molecular rotor ^{139}La-[$^{11}B_2$@$^{11}B_{18}$]-^{139}La, which are quite different from those of the individual GMs. The results have been derived for the simple model of the rotating wheel in the pseudo-rotating tubular bearing, but they are robust upon extensions to models for all vibrational degrees of freedom.[17] The present example should stimulate the search for analogous changes of the properties of other tubular, and possibly also non-tubular, molecular rotors with multiple GMs, from the individual GM_k to the quantum mechanical unified system of the interacting GMs. By analogy, this should reveal (i) structural changes, (ii) the shaping of symmetric molecular tops, (iii) the elevation of the symmetry, and (iv) the formation of energy bands.

The present derivation proceeds from the reference GMs to the quantum mechanical unified structure of the rotor. Turning the table, one may ask whether one could start from the unified image to reconstruct the GMs. The answer is "no": according to ref. ref. 15, the localized wave functions $\Psi_{k0}(\varphi)$ for GM_k could be constructed as the superposition of the delocalized $\Psi_{0l}(\varphi)$, but each spatial $\Psi_{0l}(\varphi)$ must be multiplied with a nuclear spin wave function with different IRREPs. This means that the wave functions $\Psi_{0l}(\varphi)$ of the quantum mechanical unified rotor belong to different nuclear spin isomers, *i.e.*, they must not be superimposed. To resume, the key discovery of this Communication is that the unified quantum mechanical structures of the spin-isomeric tubular rotor states are observable. However, their properties (geometry, symmetry, the type of molecular top, and the vibrational levels) are different from those of the individual GMs. These GMs cannot be observed.

Author contributions

This project was initiated by S.-D. Li who suggested the model tubular rotor and provided continuous advice. Y. Man developed the concept and wrote the zero-order draft. X.-Q. Lu contributed the results for the 18 equivalent GMs. Y. Yang developed the method and Y. Xu calculated the rotational/pseudo-rotational wave functions and energies, first for the 18 GMs and then for the unified system. V. Ruß prepared the figures of the unified system. All co-authors contributed to the final version of the manuscript.

Conflicts of interest

There are no conflicts of interest to declare.

Acknowledgements

The authors are grateful to Professors G. Buntkowski (Darmstadt) and M. Schnell (Hamburg and Kiel) for pointing to.Ref. 30–32 This work profits from financial support, in part by the National Key Research and Development Program of China (2017YFA0304203), the National Natural Science Foundation of China (Grant No. 21720102006, 21973057, and 11904215), the Program for Changjiang Scholars and Innovative Research Team (IRT_17R70), the 111 project (Grant No. D18001), the Fund for Shanxi 1331 Project Key Subjects Construction, and the Hundred Talent Program of Shanxi Province.

Notes and references

1 X.-Q. Lu, Q. Chen, X. X. Tian, Y. W. Mu, H. G. Lu and S.-D. Li, *Nanoscale*, 2019, **11**, 21311.
2 W. L. Li, T. Jian, X. Chen, H. R. Li, T. T. Chen, X. M. Luo, S.-D. Li, J. Li and L. S. Wang, *Chem. Commun.*, 2017, **53**, 1587.
3 H. R. Li, M. Zhang, M. Yan, W. Y. Zan, X. X. Tian, Y. W. Mu and S.-D. Li, *J. Cluster Sci.*, 2020, **31**, 331.
4 J. O. C. Jiménez-Halla, R. Islas, T. Heine and G. Merino, *Angew. Chem., Int. Ed.*, 2010, **49**, 5668.
5 W. Huang, A. P. Sergeeva, H. J. Zhai, B. B. Averkiev, L. S. Wang and A. I. Boldyrev, *Nat. Chem.*, 2010, **2**, 202.
6 G. Martínez-Guajardo, A. P. Sergeeva, A. I. Boldyrev, T. Heine, J. M. Ugalde and G. Merino, *Chem. Commun.*, 2011, **47**, 6242.
7 J. Zhang, A. P. Sergeeva, M. Sparta and A. N. Alexandrova, *Angew. Chem., Int. Ed.*, 2012, **51**, 8512.
8 A. P. Sergeeva, I. A. Popov, Z. A. Piazza, W. L. Li, C. Romanescu, L. S. Wang and A. I. Boldyrev, *Acc. Chem. Res.*, 2014, **47**, 1349.
9 Y. J. Wang, X. Y. Zhao, Q. Chen, H. J. Zhai and S.-D. Li, *Nanoscale*, 2015, **7**, 16054.
10 S. Jalife, L. Liu, S. Pan, J. L. Cabellos, E. Osorio, C. Lu, T. Heine, K. J. Donald and G. Merino, *Nanoscale*, 2016, **8**, 17639.
11 M. R. Fagiani, X. Song, P. Petkov, S. Debnath, S. Gewinner, W. Schöllkopf, T. Heine, A. Fielicke and K. R. Asmis, *Angew. Chem., Int. Ed.*, 2017, **56**, 501.
12 S. Pan, J. Barroso, S. Jalife, T. Heine, K. R. Asmis and G. Merino, *Acc. Chem. Res.*, 2019, **52**, 2732.
13 X.-Q. Lu, Z. Wei and S.-D. Li, *J. Cluster Sci.*, 2021, DOI: 10.1007/s10876-021-02072-x.
14 Y. Yang, D. Jia, Y. J. Wang, H. J. Zhai, Y. Man and S.-D. Li, *Nanoscale*, 2017, **9**, 1443.
15 T. Grohmann and J. Manz, *Mol. Phys.*, 2018, **116**, 2538.
16 T. Grohmann, D. Haase, D. Jia, J. Manz and Y. Yang, *J. Chem. Phys.*, 2018, **149**, 184302.
17 Y. Xu, H. Wang, Y. Yang, C. Li, L. Xiao and S. Jia, *RSC Adv.*, 2021, **11**, 3613.
18 G. S. Kottas, L. I. Clarke, D. Horinek and J. Michl, *Chem. Rev.*, 2005, **105**, 1281.
19 B. L. Feringa, *Angew. Chem., Int. Ed.*, 2017, **56**, 11060.
20 T. Akutagawa, H. Koshinaka, D. Sato, S. Takeda, S. I. Noro, H. Takahashi, R. Kumai, Y. Tokura and T. Nakamura, *Nat. Mater.*, 2009, **8**, 342.
21 Y. Feng, M. Ovalle, J. S. W. Seale, C. K. Lee, D. J. Kim, R. D. Astumian and J. F. Stoddart, *J. Am. Chem. Soc.*, 2021, **143**, 5569.
22 L. S. Wang, *Int. Rev. Phys. Chem.*, 2016, **35**, 69.
23 T. Jian, X. Chen, S.-D. Li, A. I. Boldyrev, J. Li and L. S. Wang, *Chem. Soc. Rev.*, 2019, **48**, 3550.
24 V. V. Nefedova, A. I. Boldyrev and J. Simons, *J. Chem. Phys.*, 1993, **98**, 8801.
25 W. L. Li, T. T. Chen, D. H. Xing, X. Chen, J. Li and L. S. Wang, *Proc. Natl. Acad. Sci. U. S. A.*, 2018, **115**, E6972.
26 T. T. Chen, W. L. Li and J. Li, and L. S, *Chem. Sci.*, 2019, **10**, 2534.
27 Z. Y. Jiang, T. T. Chen, W. J. Chen, W. L. Li, J. Li and L. S. Wang, *J. Phys. Chem. A*, 2021, **125**, 2622.
28 T. T. Chen, W. L. Li, W. J. Chen, J. Li and L. S. Wang, *Chem. Commun.*, 2019, **55**, 7864.
29 T. T. Chen, W. L. Li, W. J. Chen, X. H. Yu, X. R. Dong, J. Li and L. S. Wang, *Nat. Commun.*, 2020, **11**, 2766.
30 W. Caminati and J.-U. Grabow, *J. Am. Chem. Soc.*, 2006, **128**, 854.
31 H. C. Gottschalk, A. Poblotzki, M. Fatima, D. A. Obenchain, C. Pérez, J. Antony, A. A. Auer, L. Baptista, D. M. Benoit and G. Bistoni, *et al.*, *J. Chem. Phys.*, 2020, **152**, 164303.
32 A. J. Horsewill, *Prog. Nucl. Magn. Reson. Spectrosc.*, 1999, **35**, 359.